JOURNAL OF COMPUTATIONAL PHYSICS **132,** 312–326 (1997)
ARTICLE NO. CP965638

# Robust Algorithms for Solving Stochastic Partial Differential Equations

M. J. Werner* and P. D. Drummond†

*NTT Basic Research Laboratories, 3-1 Morinosato-Wakamiya, Atsugi-shi, Kanagawa, 243-01 Japan; and †Department of Physics, University of Queensland, St. Lucia, 4072, Brisbane, Australia
E-mail: *werner@will.brl.ntt.co.jp

Received January 18, 1996; revised December 4, 1996

A robust semi-implicit central partial difference algorithm for the numerical solution of coupled stochastic parabolic partial differential equations (PDEs) is described. This can be used for calculating correlation functions of systems of interacting stochastic fields. Such field equations can arise in the description of Hamiltonian and open systems in the physics of nonlinear processes, and may include multiplicative noise sources. The algorithm can be used for studying the properties of nonlinear quantum or classical field theories. The general approach is outlined and applied to a specific example, namely the quantum statistical fluctuations of ultra-short optical pulses in $\chi^{(2)}$ parametric waveguides. This example uses a non-diagonal coherent state representation, and correctly predicts the sub-shot noise level spectral fluctuations observed in homodyne detection measurements. It is expected that the methods used will be applicable for higher-order correlation functions and other physical problems as well. A stochastic differencing technique for reducing sampling errors is also introduced. This involves solving nonlinear stochastic parabolic PDEs in combination with a reference process, which uses the Wigner representation in the example presented here. A computer implementation on MIMD parallel architectures is discussed. 

## I. INTRODUCTION

Stochastic partial differential equations are a class of differential equations with important applications. Stochasticity in the description of physical systems can arise from both nonlinear processes and external noise sources. These equations provide a description of interesting and complex physical processes involving interacting fields [1]. The system may be closed or interacting with reservoirs, and the stochastic equations, if derived from an underlying Fokker–Planck equation, may have delta-correlated noise sources. A generic form of the stochastic differential equation or SDE [2, 3] addressed here is:

$$\frac{\partial}{\partial t}\boldsymbol{\phi}(t,\boldsymbol{x}) = \mathbf{L}[\boldsymbol{\phi}] + \mathbf{A}[\boldsymbol{\phi}] + \mathbf{B}[\boldsymbol{\phi}]\cdot\boldsymbol{\eta}(t,\boldsymbol{x}), \quad (1.1)$$

where $\boldsymbol{\phi}$ is an $M$-dimensional complex field vector, $\mathbf{L}$ represents some linear partial differential operators, $\mathbf{A}$ is the nonlinear evolution, and $\mathbf{B}$ is the $M \times N$ dimensional noise term, which is a functional of $\boldsymbol{\phi}$, and multiplies an $N$ dimensional real or complex Gaussian-distributed stochastic field $\boldsymbol{\eta}$. All terms in these equations are assumed to be evaluated at the same point in the independent variable $t$. The functional notation $[\boldsymbol{\phi}]$ denotes an arbitrary functional dependence on the fields $[\boldsymbol{\phi}]$, not necessarily evaluated at the same location x (even for field theories derived from local interactions), generically denoted as $\boldsymbol{x}$. The stochastic fields $\boldsymbol{\eta}(t,\boldsymbol{x})$ are generally delta-correlated in $t$, although not always in $\boldsymbol{x}$, so that

$$\begin{aligned}\langle \eta_i(t,x)\eta_{i'}(t',\boldsymbol{x}')\rangle &= \delta(t-t')C_{ii'}(x,\boldsymbol{x}')\\ \langle \eta_i(t,x)\eta_i^*(t',\boldsymbol{x}')\rangle &= \delta(t-t')C_{ii'}(x,\boldsymbol{x}').\end{aligned} \quad (1.2)$$

One of the most well-known examples of this type of stochastic partial differential equation is the time-dependent Ginsburg–Landau [4] equation with a stochastic source. This is commonly used to describe systems with critical-point phase-transitions, like super-fluids, lasers, and similar physical systems. The stochastic equation has the form (for a single field $\phi$) of

$$\frac{\partial\phi}{\partial t}(t,\boldsymbol{x}) = \mu\nabla_{\boldsymbol{x}}^2\phi + A\phi(1-|\phi|^2) + B\eta(t,\boldsymbol{x}), \quad (1.3)$$

where the complex stochastic field $\eta(t,\boldsymbol{x})$ is equivalent to two uncorrelated real Gaussian stochastic fields with equal variances. Thus, the only non-vanishing correlations of the complex noise fields in this case, are

$$\langle \eta(t,\boldsymbol{x})\eta^*(t',\boldsymbol{x}')\rangle = \delta(t-t')\delta^{(n)}(\boldsymbol{x}-\boldsymbol{x}'). \quad (1.4)$$

Here the transverse variable $\boldsymbol{x}$ is defined in an n-dimensional real space, and the stochastic noise sources are delta-correlated in all space-time dimensions. This is generally only an approximation: the above equation is often obtained as a limiting form, valid when all other time and



0021-9991/97 $25.00

distance scales are much larger than the correlation times and correlation lengths of the stochastic term. In this type of situation, it is most appropriate to use the Stratonovich form of Eq. (1.1), and we will use this type of stochastic integral throughout.

As well as treating the usual classical field systems, the set of equations given by Eq. (1.1) can be used to describe the evolution of interacting boson quantum fields [5]. The ability to describe the dynamics of quantum fields using appropriate stochastic processes has become an important tool in understanding interacting boson systems. These include the dynamics of quantum solitons [6], parametric amplifiers [7], and possibly even Bose–Einstein condensates [8]. For these reasons, we introduce an example to illustrate the stochastic techniques which comes from the nonlinear quantum optics of two fields with a nonlinear parametric coupling. This has applications to the propagation of intense pulses in nonlinear waveguides. The coherent-state representations described in the example given here therefore illustrate an important technique for solving systems with large numbers of interacting bosons. The numerical methods employed to solve the resulting differential equations provide the background to enable the reader to adapt the techniques to other systems.

A number of algorithms are known for solving problems involving ordinary stochastic differential equations [9, 10]. In general, since the stochastic term is usually non-differentiable, strategies that are appropriate for ordinary differential equations need modification in the case of stochastic equations. Similarly, techniques that might work very successfully in non-stochastic partial differential equations, may not be applicable in stochastic partial differential equations, for the same reason. The work presented in this paper is formally derived from a semi-implicit stochastic method [9], which has proved successful in treating ordinary stochastic differential equations owing to its good stability properties, combined with a relatively low discretization and sampling error. In essence, we combine the idea of split operators, which are frequently used to solve partial differential equations [11], with a semi-implicit stochastic method. This general approach has been used to derive existence theorems for stochastic partial differential equations [12], and is more robust in terms of stability than Euler techniques [13] discussed in the recent literature.

We also introduce some further innovations that are useful in practical implementations of partial stochastic differential equations. Stochastic differencing techniques can be employed when a given nonlinear problem is closely related to a simpler equation that can be treated using other techniques. The purpose of stochastic differencing is to reduce sampling errors by focusing the stochastic method on the difference field, rather than the total field. At low stochastic noise levels, a deterministically efficient solution scheme is obtained by combining two different integration step sizes, giving a scheme estimated to be at best fourth-order in the deterministic part. Finally, we introduce methods to solve the coupled nonlinear stochastic partial differential equations using distributed computing techniques involving message-passing that produce the desired ensemble averages. As an example, improvements in implementation are demonstrated via the use of stochastic trajectories in parallel, with the PVM (Parallel Virtual Machine) public-domain message-passing library [14].

## II. IMPLICIT PROPAGATION ALGORITHMS

### A. *Stochastic Differential Equations*

The numerical solution of stochastic differential equations has generally received less attention in the literature than has the equivalent problem with non-stochastic sources. In particular, the limit of small step-size is generally not the same in the two cases, since the standard deviation of the integrated noise source increases relative to the step-size in this limit. The reason for this is that the noise-sources in the equations we treat here are infinitely wide-band. This results in problems with using the normal arguments about continuity and differentiability of terms in the equations.

As a well-known illustration of this, we note that there are two forms of stochastic calculus in common use. In one, all derivatives are calculated at the current point in time, prior to a step forward. This is called Ito calculus. In the second, all derivatives are calculated implicitly, at the center of a step forward in time. This is called Stratonovich calculus. Unlike conventional differential equations, these two procedures do not result in identical limiting equations. Instead, they give rise to generally quite different looking equations in the small step-size limit. The first form is often used by mathematicians, as it has some useful theoretical properties. To many physicists, the second form is a preferred one, as it arises as the natural limit of a set of equations driven with colored noise sources, in the limit of large bandwidth. We note that it is always possible to transform from one type of calculus to the other.

As well as having conceptual advantages for the physicist, the Stratonovich calculus also has the virtue that variable-changes simply follow the rules of usual calculus. Accordingly, we will use this stochastic calculus throughout. This does not rule out Ito equations, but rather means they should first be transformed to the Stratonovich form.

The simplest type of SDE has no partial derivatives, and can be written in Stratonovich calculus as

$$\frac{\partial}{\partial t}\mathbf{x}(t) = \mathbf{A}(t, \mathbf{x}) + \mathbf{B}(t, \mathbf{x}) \cdot \boldsymbol{\zeta}(t), \tag{2.1}$$

where

$$\langle \zeta_i(t)\zeta_{i'}(t')\rangle = \delta_{i,i'}\delta(t-t'). \tag{2.2}$$

This equation can be treated as an ordinary differential equation with continuous, differentiable source terms, provided an infinite bandwidth limit is taken at the end of the calculation. However, the limit of infinite bandwidth is essential, and must be utilized *prior* to the limit of small step-size. With this in mind, time is divided into a lattice of discrete points $t_j$. The derivative term for each step from $t_j$ to $t_{j+1}$ can be evaluated by approximating the variable $\mathbf{x}$ using a Taylor expansion around some point $\bar{t}_j = (1-\varepsilon)t_j + \varepsilon t_{j+1}$. Next, the resulting approximate equation is solved in the time interval $t_j$ to $t_{j+1}$, with initial condition $\mathbf{x} = \mathbf{x}_j = \mathbf{x}(t_j)$. If a first-order Taylor expansion is used, the equations that result are exactly soluble in differential form; they result [9] in a family of numerical algorithms that are parameterized by $\varepsilon$. Each algorithm generated this way has both a strongly convergent form (which includes second-order correlations of the noise terms), and an associated weakly convergent form, which only converges stochastically, on averaging over an ensemble.

One commonly used algorithm is the explicit Milstein [15] form, with $\varepsilon = 0$, so that the functions are evaluated at the starting-point:

$$\begin{aligned}\Delta x_{i,j} = A_i(t_j,\mathbf{x}_j)\Delta t + \sum_n B_{in}(t_j,\mathbf{x}_j)\Delta W_{n,j} \\ + \sum_n\sum_{n'} C_{inn'}(t_j,\mathbf{x}_j)\Delta W_{nn'j}.\end{aligned} \tag{2.3}$$

Here the novel features are the noise integrals, defined by

$$\Delta W_{n,j} = \int_{t_j}^{t_{j+1}} \zeta_n(t)dt, \tag{2.4}$$

and the time-ordered noise correlations, defined by

$$\Delta W_{nn',j} = \int_{t_j}^{t_{j+1}}\int_{t}^{t_{j+1}} \zeta_n(t)\zeta_n'(t')dt'dt. \tag{2.5}$$

In addition, there is a stochastic coefficient, given by

$$C_{inn'}(t_j,\mathbf{x}_j) = \sum_{i'} B_{i'n}(t_j,\mathbf{x}_j)\frac{\partial}{\partial x_{i'}}B_{in'}(t_j,\mathbf{x}_j). \tag{2.6}$$

If the stochastic correction term is ensemble-averaged a weakly-convergent algorithm is regained:

$$\Delta x_{i,j} = A_i^{ITO}(t_j,\mathbf{x}_j)\Delta t + \sum_n B_{in}(t_j,\mathbf{x}_j)\Delta W_{n,j}. \tag{2.7}$$

Here the deterministic term $\mathbf{A}$ is now replaced by the deterministic term of the Ito [16] calculus, which is

$$A_i^{\mathrm{ITO}}(t,\mathbf{x}) = A_i(t,\mathbf{x}) + \frac{1}{2}\sum_n C_{inn}(t,\mathbf{x}). \tag{2.8}$$

This relationship demonstrates the operational meaning of the Ito calculus; it is equivalent to a weakly convergent explicit Euler algorithm for the stochastic equation. Both these explicit algorithms are often unstable numerically, as they do not correspond to efficient techniques for integrating the deterministic part of the equation. Thus, they are particularly unsuitable for stiff numerical problems. The weakly convergent, or Ito–Euler method, has the additional disadvantage that weak convergence often results in a large sampling error.

An alternative technique within this general class of Taylor-expansion methods is the semi-implicit technique obtained when $\varepsilon = 1/2$. Once more there are both weakly and strongly convergent methods. For a large class of stochastic processes with commutative noise (i.e., $C_{inn'} = C_{in'n}$), the weakly and strongly convergent derivations give identical algorithms, with

$$\Delta x_{i,j} = A_i(\bar{t}_j,\bar{\mathbf{x}}_j)\Delta t + \sum_n B_{in}(\bar{t}_j,\bar{\mathbf{x}}_j)\,\Delta W_{n,j}, \tag{2.9}$$

where the derivative terms on the right-hand side are all evaluated at the midpoint in time: $\bar{t}_j = (t_j + t_{j+1})/2$. Since the original approximation for $\mathbf{x}$ involved linearizing in the interval in question, the midpoint value $\bar{\mathbf{x}}_j$ is then obtained by an implicit equation:

$$\bar{\mathbf{x}}_j = (\mathbf{x}_j + \mathbf{x}_{j+1})/2 = \mathbf{x}_j + \Delta\mathbf{x}_j/2. \tag{2.10}$$

Thus, the equation for the time-evolution at the $j$th time step is now an implicit one, which involves solving for $\bar{\mathbf{x}}_j$. This can be carried out in a number of ways, although simple iteration is often the easiest in practical examples.

### B. *Partial Stochastic Differential Equations*

In general, partial stochastic differential equations can be treated in an exactly analogous way to ordinary stochastic differential equations, simply by expanding the fields to be integrated in an appropriate basis set of mode functions. In this way, a new family of algorithms can be generated, corresponding to the explicit and implicit forms treated above. It is necessary to decide precisely which type of mode expansion to use, in order to specify the algorithm. An obvious first choice is to use a wavelet basis,

consisting of square modes $U(\mathbf{x} - \bar{\mathbf{x}}_m)$ centered on a transverse lattice of points $\bar{\mathbf{x}}_m$, so that

$$\phi_i(t, \mathbf{x}) \simeq \sum_m U(\mathbf{x} - \bar{\mathbf{x}}_m)\overline{\phi}_i(t, \bar{\mathbf{x}}_m). \tag{2.11}$$

Each ordinary stochastic equation algorithm can then be rewritten in terms of the wavelet basis, to give a partial differential equation algorithm. The new ingredient is that the transverse cells must be averaged over at each step. Choosing the semi-implicit algorithm, this leads to an equation for the mean increment after cell-averaging:

$$\begin{aligned}\Delta\overline{\boldsymbol{\phi}}(t_j, \bar{x}_m) = (\mathbf{L}_{mm'} \cdot \boldsymbol{\phi}_{jm'} + \mathbf{A}[\boldsymbol{\phi}_{jm}])\Delta t \\ + \mathbf{B}[\boldsymbol{\phi}_{jm}] \cdot \Delta \boldsymbol{W}_{jm}.\end{aligned} \tag{2.12}$$

Here the term $\mathbf{L}_{mm'}$ is simply the transverse discretization of the linear partial differential operator. If the cell volume is written as

$$V(\Delta\mathbf{x}_m) = \Delta x_{1m}\Delta x_{2m} \ldots, \tag{2.13}$$

then the transverse noise integrals are

$$\Delta W_{n,jm} = \frac{1}{V(\Delta\mathbf{x}_m)} \int_{t_j}^{t_{j+1}} \int_{x_m}^{x_{m+1}} \eta_n(t, \mathbf{x})\, dt\, d\mathbf{x}. \tag{2.14}$$

The midpoint fields can then be estimated to lowest order by the implicit formula

$$\boldsymbol{\phi}_{jm} \simeq (\overline{\boldsymbol{\phi}}(t_j, \bar{x}_m) + \overline{\boldsymbol{\phi}}(t_{j+1}, \bar{x}_m))/2. \tag{2.15}$$

The above result defines a semi-implicit algorithm, involving the evaluation of a set of nonlinear equations at each step.

In order to evaluate the semi-implicit step numerically, it is often most convenient to start with an explicit Ito–Euler integration step of length $\Delta t/2$. This simple method is rather unstable for stochastic differential equations in general [9], and should not therefore be used on its own. Accordingly, to improve on the Ito–Euler integration step an iterated root-finding mechanism can be used. One defines the $(n + 1)$st iterate as

$$\begin{aligned}\boldsymbol{\phi}_{jm}^{(n+1)} = \overline{\boldsymbol{\phi}}_j(t_j, \bar{x}_m) + [(\mathbf{L}_{mm'} \cdot \boldsymbol{\phi}_{jm'}^{(n)} + \mathbf{A}[\boldsymbol{\phi}_{jm}^{(n)}])\Delta t \\ + \mathbf{B}[\boldsymbol{\phi}_{jm}^{(n)}] \cdot \Delta\mathbf{W}_{jm}]/2,\end{aligned} \tag{2.16}$$

where initially, $\boldsymbol{\phi}_{jm}^{(0)} = \overline{\boldsymbol{\phi}}(t_j, \bar{\mathrm{x}}_m)$. About $n = 3$ or $n = 4$ iterations are usually sufficient for convergence at small step-sizes. The final nonlinear step operator acting on a field $\overline{\boldsymbol{\phi}}$ is

$$\overline{\boldsymbol{\phi}}(t_{j+1}, \bar{x}_m) = 2\boldsymbol{\phi}_{jm}^{(n)} - \overline{\boldsymbol{\phi}}(t_j, \bar{x}_m). \tag{2.17}$$

This is used in preference to a direct Newton root-finding method requiring evaluation of steps involving the Jacobian of the drift and noise terms, since this would add considerable complexity to the algorithm.

## III. FOURIER TRANSFORM METHODS

### A. *Linear Propagation*

An alternative basis is the Fourier expansion basis, which has the advantage that the set of functions employed has no discontinuities. While this can simply be used directly as in the above section, it is also possible to use a Fourier expansion in an interaction picture approach, which results in a rather efficient implementation. We will restrict our attention here to (1 + 1) dimensional equations. Higher dimensional problems can be treated by using higher dimensional FFTs or eigenfunction expansions. Assuming that $\mathbf{L}$ is diagonal in the field indices, the linear evolution for each vector field component can be expressed in a standard form as

$$\mathbf{L}[\phi(t, x)]_i = \sum_{n=0}^{n_{max}} i^{n+1} \frac{\beta_i^{(n)}}{n!} \frac{\partial^n}{\partial x^n} \phi_i(t, x). \tag{3.1}$$

A Fourier transform basis is defined as

$$\begin{aligned}\tilde{\boldsymbol{\phi}}(t, k) &= \int_{-L/2}^{L/2} \boldsymbol{\phi}(t, x) e^{ikx}\, dx \\ \boldsymbol{\phi}(t, x) &= \frac{1}{L} \sum \boldsymbol{\phi}(t, k) e^{-ikx},\end{aligned} \tag{3.2}$$

where the Fourier transform operator is denoted $\mathscr{T}$.

The boundary terms which can occur in the Fourier transform are usually assumed to be negligible. This requires the field and its first derivative in $x$ to be small on the boundary at $x = \pm L/2$: or else $\boldsymbol{\phi}$ must be periodic, since typical numerical implementations of Fourier transforms involve a finite domain. Absorbing boundaries can be used to prevent noise from wrapping around the boundaries. In the case of some types of representation of quantum fields, noise sources must then be added, to preserve commutation relations whenever the fields explicitly contain vacuum noise. In practice, Fourier transforms are computed using a finite sample discrete Fourier transform which implicitly enforces periodicity, and also introduces a momentum cutoff, corresponding to a cell-size of $\Delta x$. The corresponding discrete Fourier transform operator is denoted $\mathscr{T}_{\Delta x}$.

Equation (3.2) forms the basis of a propagator for the linear evolution by direct integration, allowing a linear

evolution operator $\mathbf{U_L}(t) = \mathscr{T}^{-1}[\mathbf{P_L}(t)\mathscr{T}[\boldsymbol{\phi}]]$ to be constructed, where the propagator in Fourier space is

$$\{\mathbf{P_L}(t)\}_i = \exp\left[i\sum_{n=0}^{n_{max}} \frac{\beta_i^{(n)} k^n}{n!} t\right] = e^{i\theta_i(k)t}. \tag{3.3}$$

Thus, $\mathbf{P_L}(t)$ is the exact linear propagator for the evolution of the transformed field at wavevector $k$, under the action of the linear operator $\mathbf{L}$. In typical physical applications, this may include the linear dispersion of the propagation equation along with phase-mismatch and damping.

The existence of this solution means that the original equation can be rewritten in a type of "interaction picture" relative to a reference time $t_0$ (using field theory terminology), as

$$\frac{\partial}{\partial t}\tilde{\boldsymbol{\phi}}_I = \mathbf{P_L}(t_0 - t)\mathscr{T}[\mathbf{A}[\boldsymbol{\phi}(t)] + \mathbf{B}[\boldsymbol{\phi}(t)]\cdot\boldsymbol{\eta}(t,\boldsymbol{x})], \tag{3.4}$$

where the linear term is eliminated through the replacement of $\boldsymbol{\phi}$ by the interaction picture field $\tilde{\boldsymbol{\phi}}_I$, so that $\boldsymbol{\phi}(t) = \mathscr{T}^{-1}[\mathbf{P_L}(t - t_0)\tilde{\boldsymbol{\phi}}_I(t)]$.

In this form, the equation can be regarded as essentially an ordinary differential equation (or integro-differential equation) which can be treated using the semi-implicit technique [9]. As stated earlier, time is divided into a lattice of discrete points $t_j$, and the derivative term for each step from $t_j$ to $t_{j+1}$ is evaluated by approximating the field on the right-hand side by its value at the midpoint in time $\bar{t}_j = (t_j + t_{j+1})/2$. In every successive step the reference time is set to $t_0 = \bar{t}_j$, so that the midpoint derivative is identical (apart from the linear terms) in either picture of the evolution.

## B. *Transverse Lattice*

The interaction picture presented above does not take into account the fact that a finite lattice of modes $k_l$ must be used in a practical numerical implementation, together with an equivalent lattice in the $x$-domain. The fields are integrated with a momentum cut-off, and therefore can be effectively sampled at each lattice midpoint. However, the stochastic term has no intrinsic momentum cutoff, and must be treated more carefully. In order to treat this, we introduce a discrete Fourier transform defined on a discrete transverse lattice with lattice spacing $\Delta x$, where

$$\begin{aligned}\mathscr{T}_{\Delta x}[\phi_i](t,k_l) &= \Delta x \sum e^{ik_l\bar{x}_m}\phi_i(t,\bar{x}_m)\\ \mathscr{T}_{\Delta x}[\overline{\eta}_n](t,k_l) &= \Delta x \sum e^{ik_l\bar{x}_m}\overline{\eta}_{n,m}(t)\\ &= \int_{-L/2}^{L/2}\eta_n(t,x)e^{ik_l x}\,dx.\end{aligned} \tag{3.5}$$

If the original noise terms are delta-correlated in space, then the momentum-space noise terms are correlated according to

$$\langle\overline{\eta}_n(t,k_l)\overline{\eta}_{n'}(t',k_l')\rangle = L\delta_{n,n'}\delta(t-t')\delta_{k_l,-k_{l'}}. \tag{3.6}$$

As usual, we choose the $x$-lattice and $k$-lattice to be conjugate to each other, to allow inverse Fourier transforms to exist. Nonlinear terms involving products in the $x$-domain are transformed to convolutions in the Fourier domain. These must be truncated to a finite lattice, which is achieved by evaluating the $x$-domain products only at the conjugate lattice points. Similarly, the noise terms must be averaged over each cell.

This leads to an equation for the mean increment in the form

$$\begin{aligned}\Delta\tilde{\boldsymbol{\phi}}_I(t_j,k_l) = \int_{t_j}^{t_{j+1}} dt\,\mathbf{P_L}(\bar{t}_j - t)\mathscr{T}_{\Delta x}[\mathbf{A}[\boldsymbol{\phi}_{jm}]\\ + \mathbf{B}[\boldsymbol{\phi}_{jm}]\cdot\overline{\boldsymbol{\eta}}_m(t)],\end{aligned} \tag{3.7}$$

where $\boldsymbol{\phi}_{jm} = \boldsymbol{\phi}(\bar{t}_j,\bar{x}_m) = \boldsymbol{\phi}_I(\bar{t}_j,\bar{x}_m)$. This equation can be readily simplified by noting that the temporal average of the deterministic part is $\Delta t(k) = \Delta t\,\mathrm{sinc}(\theta_m(k)\Delta t/2)$. Here it should be clear that for small enough step-size, $\Delta t(k) = \Delta t$. The effect of the temporal integral is to filter large momentum components in the nonlinear response, when the step-size is large. Similarly, the average of the stochastic term is

$$\Delta W_{i,jm}^T(k) = \sum_n \int_{t_j}^{t_{j+1}} dt e^{i\theta_i(k)(\bar{t}_j - t)}B_{in}[\boldsymbol{\phi}_{jm}]\overline{\eta}_{n,m}(t). \tag{3.8}$$

This also has a filtering effect; effectively, a random phase is applied to each Fourier-transformed noise component. This filters the phase-dependent noise terms, but has no effect on phase-independent noise.

The complete interaction picture result is

$$\Delta\tilde{\boldsymbol{\phi}}_I(t_j,k_l) = \mathscr{T}_{\Delta x}[\mathbf{A}[\boldsymbol{\phi}(\bar{t}_j,\bar{x}_m)]]\Delta t(k_l) + \Delta\mathbf{W}_{jm}^T(k_l). \tag{3.9}$$

For simplicity, it is often preferable to employ a small step-size $\Delta t$, so that for $\Delta t\theta(k_{max}) \ll 1$ the filtering terms are eliminated. More precisely, at small step-size, the resulting sinc function gives corrections of order $(\Delta t)^3$, which can be neglected. The noise expression then reduces to $\Delta W_{i,jm}^T(k) = \sum_n B_{in}[\boldsymbol{\phi}_{jm}]\Delta W_{n,jm}$, where $\Delta\mathbf{W}_{jm}$ is a cell-averaged noise, as defined in Eq. (2.14).

In this case, the step can be written in an approximate form applicable in the time-domain, in terms of the central

fields $\boldsymbol{\phi}_{jm}$ in each lattice cell, as

$$\boldsymbol{\phi}_I(t_j + \Delta t, \bar{x}_m) = \boldsymbol{\phi}_I(t_j, \bar{x}_m) + \mathbf{A}[\boldsymbol{\phi}_{jm}]\Delta t + \mathbf{B}[\boldsymbol{\phi}_{jm}] \cdot \Delta \mathbf{W}_{jm}. \tag{3.10}$$

In addition, there must be a specification of how to evaluate the midpoint fields. For ease of implementation, we choose to estimate the midpoint fields to lowest order by averaging the interaction picture fields, so that $\boldsymbol{\phi}_{jm} \simeq [\overline{\boldsymbol{\phi}}_I(t_j, \bar{x}_m) + \overline{\boldsymbol{\phi}}_I(t_{j+1}, \bar{x}_m)]/2$. The overall result defines a semi-implicit algorithm at small step-size; more precise treatments should include the transverse filters obtained above. In practice, it is necessary to evaluate a set of nonlinear equations for each step. This can be achieved in a number of ways, although iterative techniques are usually convenient.

Generally the nonlinear field term $\mathbf{A}$ is evaluated in the $x$-domain as indicated above, although field convolutions involving $x$ can be efficiently evaluated using the convolution property of Fourier transforms. For example, the ability to perform calculations in the Fourier domain can be used as a convenient method for including the effects of a nonlinear response that is non-local in $x$. This form appears in the theory of polariton propagation in Raman active waveguides as used to describe optical solitons in silica fiber [6]. Nonlinear processes often result in stochastic equations which have multiplicative noise sources. It is usually simplest to evaluate the multiplicative noise in the $x$-domain along with any nonlinear drift components. However, it is also possible to include the noise in the Fourier domain if for example the noise correlation functions are considerably simpler in the Fourier domain. Here the nonlinearity and stochasticity is included in the $x$-domain, for definiteness.

The semi-implicit step can be evaluated either exactly, if the nonlinear equations are soluble, or iteratively, if they are not. The procedure at this stage is then identical to that in Eq. (2.16), except that the differential operator $\mathbf{L}$ is omitted, due to the use of the interaction picture. This allows a more efficient implementation. The other difference is that the propagated interaction picture field is used as the initial condition, so that initially, $\boldsymbol{\phi}_{jm}^{(0)} = \overline{\boldsymbol{\phi}}_I(t_j, \bar{x}_m)$.

The final nonlinear step operator acting on a field $\overline{\boldsymbol{\phi}}_I$ in the interaction picture is

$$\begin{aligned}\overline{\boldsymbol{\phi}}_I(t_{i+1}, \bar{x}_m) &= 2\boldsymbol{\phi}_{jm}^{(n)} - \overline{\phi}_I(t_i, \bar{x}_m) \\ &= \mathbf{U}_I(\Delta t, \Delta x)[\overline{\boldsymbol{\phi}}_I(t_i, \bar{x}_m)].\end{aligned} \tag{3.11}$$

This is used in preference to a direct Newton root-finding method requiring evaluation of steps involving the Jacobian of the drift and noise terms, since this would add considerable complexity to the algorithm.

An overall semi-implicit integration step including propagation can be denoted by the total Fourier domain propagator $\mathbf{P}_{\mathscr{F}}(\Delta t, \Delta x)$, which is then of the form

$$\mathbf{P}_{\mathscr{F}}(\Delta t, \Delta x) = \mathbf{P}_{\mathbf{L}}(\Delta t/2)\mathscr{T}_{\Delta x}\mathbf{U}_I(\Delta t, \Delta x)_{\mathscr{T}\Delta x}^{-1}\mathbf{P}_{\mathbf{L}}(\Delta t/2). \tag{3.12}$$

The general approach described above allows the integration of parabolic partial differential equations with multiplicative noise. Nonlinear drift terms along with multiplicative noise in the Stratonovich form of Eq. (1.1) can be treated using the semi-implicit integration method. The method can also treat the description of interacting fields with non-Markovian reservoirs. For such systems, starting from Gaussian white noise one can generate noise sources with complicated temporal correlation functions. These can subsequently appear in multiplicative noise terms and be integrated along with the nonlinear drift terms. The method has been successfully applied to the propagation of coherent quantum solitons in silica fiber [6, 18, 19] and to the generation of non-classical light in parametric waveguides [20].

## IV. NUMERICAL ERRORS

As always, a crucial point in numerical integration is the control and estimation of numerical errors. In stochastic differential equations (either ordinary or partial), there are two distinct types of error, namely sampling errors and discretization errors. These have quite different origins, and need to be estimated and controlled individually.

### A. *Sampling Errors*

Sampling errors are a very important part of stochastic equations, because they are often the largest single error component. In general, any fluctuating or noise-driven quantity will be very susceptible to sampling error, which is due to the estimation of correlations or moments using only a finite, rather than an infinite set of random trajectories. Here we assume that the appropriate pseudo-random numbers can be generated with ideal properties. In these calculations, the Gaussian random numbers are generated using the rectangular Box–Mueller technique, combined with a pseudo-random number generator. We used the *ranmar* routine described by Marsaglia *et al.* [21]. Even with perfect random number generators, the use of a finite ensemble of $\mathscr{N}$ trajectories typically leads to a standard deviation in the result that scales at best with $1/\sqrt{\mathscr{N}}$. This relatively slow convergence as the number of stochastic trajectories increases typically results in much larger errors than those due to discretization, which can be controlled rather well in most cases. An important aspect of sampling errors is that these are often much smaller in strongly convergent algorithms than in weakly convergent algorithms.

One way to reduce sampling errors is through the use of stochastic differencing. The concept of stochastic differencing is a very simple one, although not always possible to implement. It is sometimes the case that a given correlation function or mean value $\langle \mathscr{C}[\boldsymbol{\phi}] \rangle$ can be compared to a similar correlation evaluated from a much simpler stochastic reference process, $\boldsymbol{\phi}_R$. Provided that both $\boldsymbol{\phi}$ and $\boldsymbol{\phi}_R$ can be generated with identical stochastic noise terms, this provides a technique for reducing sampling errors through a subtraction scheme.

Instead of computing the $\mathscr{N}$-trajectory average $\langle \mathscr{C}[\boldsymbol{\phi}] \rangle_{\mathscr{N}}$ directly, the difference $\langle \mathscr{C}[\boldsymbol{\phi}] - \mathscr{C}[\boldsymbol{\phi}_{\mathscr{R}}] \rangle_{\mathscr{N}}$ is computed. Suppose that the exact value of $\langle \mathscr{C}[\boldsymbol{\phi}_{\mathscr{R}}] \rangle$ is already known, or can be calculated to high accuracy using some other technique. Then, the numerical estimate of $\langle \mathscr{C}[\boldsymbol{\phi}] \rangle$ is obtained from the obvious approximation that

$$\langle \mathscr{C}[\boldsymbol{\phi}] \rangle \simeq \langle \mathscr{C}[\boldsymbol{\phi}] - \mathscr{C}[\boldsymbol{\phi}_{\mathscr{R}}] \rangle_{\mathscr{N}} + \langle \mathscr{C}[\boldsymbol{\phi}_{\mathscr{R}}] \rangle. \tag{4.1}$$

This is not a linearization approximation, but rather an alternative to the usual sampling estimate in which the exact average over an infinite population is equated with the population average over a finite sample. The advantage of a stochastic differencing method, if applicable, is that sampling errors can be greatly reduced when the reference calculation gives very similar results to the main stochastic process of interest.

In practical terms, it is not essential that the exact value of $\langle \mathscr{C}[\boldsymbol{\phi}_{\mathscr{R}}] \rangle$ is known analytically. This is obviously preferable, but not really necessary. Instead, we will show an example in which the correlation function of the reference process is calculated by using a completely different stochastic implementation, which can be carried out more efficiently. In this case, there are two distinct and equivalent routes to computing the reference correlation. One employs a stochastic reference process, with identical stochastic noise terms to the main calculation, to allow a low-noise difference term $\langle \mathscr{C}[\boldsymbol{\phi}] - \mathscr{C}[\boldsymbol{\phi}_{\mathscr{R}}] \rangle_{\mathscr{N}}$ to be calculated. The second route to calculating the reference correlation in this case is also numerical, but carried out using a more precise technique that is only available for the high-accuracy reference calculation of $\langle \mathscr{C}[\boldsymbol{\phi}_{\mathscr{R}}] \rangle$.

### B. *Discretization Errors*

Discretization errors are caused by the finite step-size employed in the numerical lattice. As this is a complex issue in stochastic problems, the most conservative procedure is to solve the equation on two distinct lattices, using identical noise sources. Noise on the fine lattice is averaged over the $t$- and $x$-lattices to form the noise for the coarse lattice. This allows an estimate of discretization error to be obtained, without sampling error artifacts being introduced—as would occur if two independent noise-fields were employed. There are also some possible techniques for reducing the discretization error, using extrapolation methods. We note that the local discretization error [9] in the stochastic terms is of order $(\Delta t)^{3/2}$, which means that conventional extrapolation schemes must be employed with caution.

For ordinary differential equations, the second-order midpoint method can be extrapolated to zero step-size, giving an algorithm known to be fourth-order by combining results from two different step sizes [17]. We can apply the technique here at the level of the full second-order split-step form rather than at the nonlinear step only. This is useful if it is essential to reduce the deterministic propagation error, and the stochastic noise term is very small. However, this procedure will not always reduce the stochastic error, as the stochastic error is not of second order. Using the Baker–Hausdorff formula one has

$$\exp(tH_1)\exp(tH_2) = \exp\left\{ t(H_1 + H_2) + \frac{t^2}{2}[H_1, H_2] + \frac{t^3}{12}([H_1,[H_1,H_2]] + [H_2,[H_2,H_1]]) + \ldots \right\} \tag{4.2}$$

which can be used to expand the symmetrized operator $\exp(tH_1/2)\exp(tH_2)\exp(tH_1/2)$ to give

$$\exp(tH_1/2)\exp(tH_2)\exp(tH_1/2) = \exp\left\{ t(H_1 + H_2) + \frac{t^3}{3}[H_1 + H_2,[H_2,H_1]] + O(t^5) \right\}. \tag{4.3}$$

We use this as a basis for the extrapolation as

$$\mathbf{P}_{ext} = \frac{4\mathbf{P}_{\mathscr{T}}(\Delta t, \Delta x) - \mathbf{P}_{\mathscr{T}}(2\Delta t, \Delta x)}{3}. \tag{4.4}$$

To test convergence, it is useful to compare results obtained using both fine and coarse lattices. The propagators then become

$$\mathbf{P}_{coarse} = \frac{4\mathbf{P}_{\mathscr{T}}(\Delta t, \Delta x) - \mathbf{P}_{\mathscr{T}}(2\Delta t, \Delta x)}{3} \tag{4.5}$$

$$\mathbf{P}_{fine} = \frac{4\mathbf{P}_{\mathscr{T}}(\Delta t/2, \Delta x/2) - \mathbf{P}_{\mathscr{T}}(\Delta t, \Delta x/2)}{3}. \tag{4.6}$$

It should be emphasized that this particular refinement is only applicable to calculations with extremely small noise sources, so the discretization error is mostly deterministic

in origin. If the stochastic discretization error is large, it may be better to employ an extrapolation of the form

$$\mathbf{P}_{ext} = 2\mathbf{P}_{\mathscr{T}}(\Delta t, \Delta x) - \mathbf{P}_{\mathscr{T}}(2\Delta t, \Delta x). \tag{4.7}$$

This assumes that the total propagating error is proportional to the cell-size, which is consistent with addition of uncorrelated local errors each proportional to $\Delta t^{3/2}$.

## V. EXAMPLE—QUANTUM FIELD PROPAGATION IN $\chi^{(2)}$ WAVEGUIDES

Non-classical light pulses produced in dispersive nonlinear media offer the possibility for improved large bandwidth communication systems. It is necessary to study the quantum statistical properties of these systems since quantum noise can impose rather disappointing limits if poorly understood. At a more fundamental level, theoretical predictions of non-classical photon correlations provide a test of the quantum theoretic and computational methods used for describing quantum field propagation in dispersive nonlinear dielectrics, as evidenced by the prediction and observation of quantum solitons in optical fibers [6] and more recently photon number squeezing in the same system [19].

The use of quasi-probability densities in studying the quantum statistics of light has provided an important tool in understanding the dynamics of quantum noise in non-equilibrium nonlinear systems. Even for a closed Hamiltonian system, a description in terms of a stochastic process may not be necessary in order to be equivalent with quantum theory. Whether noise arises in the initial conditions and/or the evolution depends on the representation used for the density operator. Typical examples from nonlinear optics are $\chi^{(2)}$ and $\chi^{(3)}$ field interactions. In both these cases, the normal and anti-normal ordered representations have non-constant diffusion terms for the Fokker–Planck equation while the symmetrical ordering results in no diffusion term. This implies that multiplicative noise sources are required in order for the SDE description to be equivalent to the Fokker–Planck equation in the normal and anti-normal ordered cases. This noise arises from the nonlinearity of the system due to the photon transitions. In the large photon number limit, a diffusion picture is a valid one but for small photon numbers the quantum jump process from which the noise originates should be considered.

Traveling-wave parametric amplifiers are phase-sensitive amplifiers where in general three-wave mixing processes via a $\chi^{(2)}$ nonlinearity include parametric down-conversion, second-harmonic generation and effective $\chi^{(3)}$ processes via cascaded $\chi^{(2)}$ interactions. This example describes an efficient algorithm for calculating quantum statistics of parametric down-conversion. In particular, the sub-shot noise level spectral fluctuations observed in recent experiments on ultra-short optical pulsed squeezing in parametric waveguides can be calculated [20].

The traveling-wave parametric amplifier is modeled here as a nonlinear, dispersive dielectric waveguide which allows propagation in the $z$-direction in single transverse modes for both the fundamental (signal) and second harmonic (pump) and is orientated such that type I phase matching for the $\chi^{(2)}$ process is dominant. The Hamiltonian used here is the same as appears in the earlier work of Raymer *et al.* [22],

$$\begin{aligned}\hat{H} = &\sum_m \hbar\omega_m^{(1)}\hat{a}_m^{(1)\dagger}\hat{a}_m^{(1)} + \sum_m \hbar\omega_m^{(2)}\hat{a}_m^{(2)\dagger}\hat{a}_m^{(2)} \\ &- \frac{1}{3}\varepsilon_0\chi^{(2)}\int d^3x : \left[\frac{\hat{D}^{(1)}(\mathbf{x})}{\varepsilon_1} + \frac{\hat{D}^{(2)}(\mathbf{x})}{\varepsilon_2}\right]^3 :,\end{aligned} \tag{5.1}$$

where the notation : : represents normal ordering. The electric displacements $D^{(i)}(\mathbf{x})$ in the nonlinear term are expanded in terms of the boson field operators as

$$\begin{aligned}\hat{D}^{(i)}(\mathbf{x}) = i\sum_m \left(\frac{\varepsilon_j\hbar\omega_j' k_0^{(i)}}{2L}\right)^{1/2} \hat{a}_m^{(i)} u^{(i)}(\mathbf{x}) \exp(ik_m^{(i)}z) \\ + \text{(hermitean adjoint)},\end{aligned} \tag{5.2}$$

where the frequency dependence of the parameters has been kept only for the phase-shift term $\exp(ik_m^{(i)}z)$. The electric permittivity at frequencies $\omega_1$ and $\omega_2$ are given by $\varepsilon_1$ and $\varepsilon_2$. The annihilation operators $\hat{a}_m^{(i)}$ correspond to a mode with propagation constant

$$k_m^{(i)} = \left(\frac{\varepsilon_j}{\varepsilon_0}\right)^{1/2}\frac{\omega_j}{c} + m\Delta k; \qquad m = -M, ..., M \tag{5.3}$$

with mode spacing $\Delta k = 2\pi/L$. The mode volume is then defined by the normalized transverse mode function $u^{(i)}(\mathbf{x})$ and the length $L$ of the medium. Here $\mathbf{x}$ represents the transverse coordinates. The mode frequencies $\omega_m^{(i)}$ are approximate, corresponding to a second-order Taylor expansion, so that

$$\omega_m^{(i)} \approx \omega_j + (m\Delta k)\omega_j' + \frac{1}{2}(m\Delta k)^2\omega_j'', \tag{5.4}$$

where the derivatives $\omega_j'$ and $\omega_j''$ are with respect to $k$. This is easily extended to include higher-order dispersion if desired. The procedure for transforming to local field operators has been given in the work of Drummond and Carter [23]. The local field operators are defined on a lattice of length $L$ with $2M + 1$ points by

$$\hat{\alpha}_l = \frac{1}{\sqrt{2M+1}}\sum_{m=-M}^{M}\hat{a}_m^{(1)}\exp\left(\frac{i2\pi ml}{2M+1}\right) \tag{5.5}$$

so that the lattice cell denoted by $l$ corresponds to longitudinal position $z_l = l\Delta z = lL/(2M+1)$. Local operators $\hat{\beta}_l$ are defined analogously from the $\hat{a}_m^{(2)}$ operators. The Hamiltonian can be written in an interaction picture, which removes the carrier frequency oscillations, as

$$\hat{H}/\hbar = \sum_l \sum_{l'} \Delta\omega^{\alpha}_{ll'} \hat{\alpha}_l^\dagger \hat{\alpha}_{l'} + \sum_l \sum_{l'} \Delta\omega^{\beta}_{ll'} \hat{\beta}_l^\dagger \hat{\beta}_{l'} \tag{5.6}$$

$$+ \left( \frac{1}{2} i\chi^* \omega_1' \left( \frac{\omega_2'}{\Delta z} \right)^{1/2} \sum_l \hat{\alpha}_l^{\dagger 2} \hat{\beta}_l e^{-i(2k_0^{(1)} - k_0^{(2)}) z_l} + h.a \right), \tag{5.7}$$

where the definition of $\Delta\omega_{ll'}$ follows directly [23] from substituting Eq. (5.5) into Eq. (5.1) and

$$\chi = \frac{\varepsilon_0 \chi^{(2)} k_0^{(1)}}{\varepsilon_1} \left( \frac{\hbar k_0^{(2)}}{2\varepsilon_2} \right)^{1/2} \int d^2\mathbf{x} (u^{(1)}(\mathbf{x}))^2 (u^{(2)*}(x)). \tag{5.8}$$

Here the $s$-parameterized quasi-probability distributions of Cahill and Glauber [24] are used which are denoted by $W(\boldsymbol{\alpha}, \boldsymbol{\beta}; s, t)$. With these distribution functions, $s$-ordered products $\langle \{(a^\dagger)^n a^m\}_s \rangle$ can be obtained by integration in the complex plane according to

$$\langle \{(a^\dagger)^n a^m\}_s \rangle = \int (\alpha^*)^n \alpha^m W(\alpha; s, t)\, d^2\alpha. \tag{5.9}$$

The parameter $s = 1, 0, -1$ corresponds to normal, symmetric, and anti-normal ordered products and the quasi-probability distributions P, Wigner, and Q functions, respectively. The evolution equation for the $s$-parameterized quasi-probability densities are obtained from the Louiville equation for the density operator [25], and are

$$\frac{\partial}{\partial t} W(\boldsymbol{\alpha}, \boldsymbol{\beta}; s, t) = \left[ \sum_l - \frac{\partial}{\partial \alpha_l} \left( -i \sum_{l'} \Delta\omega^{\alpha}_{ll'} \alpha_{l'} + \chi_l^* \alpha_l^* \beta_l \right) \right.$$

$$+ \sum_l - \frac{\partial}{\partial \alpha_l^*} \left( +i \sum_{l'} \Delta\omega^{\alpha}_{l'l} \alpha_l^* + \chi_l \alpha_l \beta_l^* \right)$$

$$+ \sum_l - \frac{\partial}{\partial \beta_l} \left( -i \sum_{l'} \Delta\omega^{\beta}_{ll'} \beta_{l'} - \frac{1}{2} \chi_l \alpha_l^2 \right)$$

$$+ \sum_l - \frac{\partial}{\partial \beta_l^*} \left( +i \sum_{l'} \Delta\omega^{\beta}_{l'l} \beta_l^* - \frac{1}{2} \chi_l^* \alpha_l^{*2} \right)$$

$$+ \sum_l s \frac{\chi_l^*}{2} \frac{\partial^2}{\partial \alpha_l^2} \beta_l + \sum_l s \frac{\chi_l}{2} \frac{\partial^2}{\partial \alpha_l^{*2}} \beta_l^*$$

$$+ \frac{\chi_l^*}{8} (1 - |s|) \sum_l \frac{\partial^3}{\partial \alpha_l^2 \partial \beta_l^*} + \frac{\chi_l}{8}$$

$$\left. (1 - |s|) \sum_l \frac{\partial^3}{\partial \alpha_l^{*2} \partial \beta_l} \right] W(\boldsymbol{\alpha}, \boldsymbol{\beta}; s, t), \tag{5.10}$$

where $\chi_l = \chi\omega_1' \sqrt{\omega_2'/\Delta z}$ and the phase-mismatch has been incorporated into $\Delta\omega^{\beta}_{ll'}$. The above derivation of the evolution equation for $W(\boldsymbol{\alpha}, \boldsymbol{\beta}; s, t)$ relies upon the use of partial integration, and therefore assumes the distribution is sufficiently rapidly vanishing at the phase-space boundaries where $|\alpha_l|, |\beta_l| \to \infty$. This condition may not always hold at long times and small damping rates, and must be checked numerically when using phase-space distributions of this type.

## VI. STOCHASTIC FIELD EQUATIONS

A Fokker–Planck equation with second-order derivatives can be transformed to a set of stochastic differential equations, provided there is a positive semidefinite diffusion which Eq. (5.10) does not provide explicitly. However, this can be achieved in two distinct ways.

In the normally ordered (or anti-normally ordered) case, there is no third order diffusion term. In the case $s = 1$, a new representation called the positive-P representation is obtained from the above Fokker–Planck equation by the procedure of dimension-doubling, which introduces new complex variables denoted $\alpha_l^\dagger$, $(\beta_l^\dagger)$. These are not necessarily the complex conjugate of $\alpha_l(\beta_l)$ except in the mean. Thus, an evolution equation for the positive-P distribution ($s = 1$) can always be found such that it has a positive semidefinite diffusion, by using the non-uniqueness of the time development of $W(\boldsymbol{\alpha}, \boldsymbol{\beta})$ corresponding to the original master equation [26]. Given that such a diffusion matrix exists, and it is the noise correlations of the SDEs which are the important property, one can write down a convenient noise term with the appropriate correlations. There are no third order derivative terms in the case of the positive-P representation, so no additional assumptions are needed to transform the Fokker–Planck equation into stochastic equations, except the requirement of vanishing boundary terms. This can be checked numerically, simply by monitoring large-amplitude trajectories.

In the Wigner case with $s = 0$, there are no second-order derivatives (unless there is damping). Accordingly, if the third order derivatives are omitted, the equations of motion are essentially classical, and all the quantum noise enters in the initial conditions. However, the transformation to a final truncated or ''semi-classical'' equation is only approximate, since it requires the neglect of third

order derivative terms. This approximation is justified by the argument that, with large photon numbers, the neglected terms are relatively small. The large photon-number approximation is difficult to check directly, and can lead to incorrect results if higher-order correlations are calculated. One can compare results with the $s = 1$ case, since the neglect of boundary terms in the positive-P simulations is readily justified for the parameters used here. The equations do have another use, as we see later. If the pump field $\psi$ is treated classically, there are no third order terms, which allows the Wigner theory to be used as a reference calculation in a stochastic differencing approach.

Either type of equation can be transformed to treat scaled photon flux amplitudes by defining

$$\begin{aligned}\phi_l &= \alpha_l \left(\frac{\omega_1'}{\Delta z}\right)^{1/2} \Big/ \Psi_0 \\ \psi_l &= \beta_l \left(\frac{\omega_2'}{\Delta z}\right)^{1/2} \Big/ \Psi_0,\end{aligned} \tag{6.1}$$

where $\phi_l^\dagger \phi_l$ and $\psi_l^\dagger \psi_l$ equal the number of photons per second passing the $z_l$ plane for signal and pump fields, respectively, scaled by a reference photon flux $|\Psi_0|^2$.

We now transform to a co-moving frame at speed $\omega_1'$ and evaluate the terms involving $\Delta\omega_{ll'}$ which are related to the discretized first and second derivatives with respect to $z$. We retain only the first-order derivative in $z$ in the co-moving frame to give continuum equations. This is achieved by first defining $t_v = t - z/v$, $k_j'' = d^2k/d\omega^2|_{k=k_j} = -\omega_j''/v^3$, where $t$ is the time measured in the laboratory frame and $t_v$ is the time measured in the co-moving frame with speed $v = \omega_1'$. The factor $(k_0^{(2)} - 2k_0^{(1)})$ accounts for any mismatch of phase velocities, while $(1/\omega_2' - 1/\omega_1')$ accounts for group-velocity mismatch, and $k_j''$ accounts for group-velocity dispersion (GVD). Finally, these equations can be cast into the following dimensionless form,

$$\begin{aligned}\frac{\partial \phi}{\partial \xi} &= -\frac{i}{2}\,\mathrm{sgn}(k_1'')\frac{\partial^2}{\partial \tau^2}\phi + \phi^\dagger\psi + s\sqrt{\psi}\zeta(\xi,\tau) \\ \frac{\partial \phi^\dagger}{\partial \mathrm{j}} &= +\frac{i}{2}\,\mathrm{sgn}(k_1'')\frac{\partial^2}{\partial \tau^2}\phi^\dagger + \phi\psi^\dagger + s\sqrt{\psi^\dagger}\zeta^\dagger(\xi,\tau) \\ \frac{\partial \psi}{\partial \xi} &= \left[\frac{z_0}{t_0}\left(\frac{1}{\omega_1'} - \frac{1}{\omega_2'}\right)\frac{\partial}{\partial \tau} + iz_0(k_0^{(2)} - 2k_0^{(1)})\right. \\ &\quad \left. - \frac{i}{2}\frac{k_2''}{|k_1''|}\left(\frac{\omega_2'}{\omega_1'}\right)^2\frac{\partial^2}{\partial \tau^2}\right]\psi - \frac{1}{2}\phi^2\end{aligned}$$

$$\begin{aligned}\frac{\partial \psi^\dagger}{\partial \xi} &= \left[\frac{z_0}{t_0}\left(\frac{1}{\omega_1'} - \frac{1}{\omega_2'}\right)\frac{\partial}{\partial \tau} - iz_0(k_0^{(2)} - 2k_0^{(1)})\right. \\ &\quad \left. + \frac{i}{2}\frac{k_2''}{|k_1''|}\left(\frac{\omega_2'}{\omega_1'}\right)^2\frac{\partial^2}{\partial \tau^2}\right]\psi^\dagger - \frac{1}{2}\phi^{\dagger 2},\end{aligned} \tag{6.2}$$

where $\xi = z/z_0$ is the propagation distance scaled by $z_0$ and $\tau = t_v/t_0$ is the scaled time in the co-moving frame. Here $z_0 = |\chi\Psi_0|^{-1}$ is the classical undepleted pump gain length and $t_0 = \sqrt{z_0 k_1''}$ is the inverse phase-matching bandwidth when $\Psi_0$ is the initial peak value of $\Psi$. The noise correlation is

$$\langle \zeta(\xi,\tau)\zeta(\xi',\tau')\rangle = \frac{1}{\bar{n}}\,\delta(\xi - \xi')\delta(\tau - \tau'), \tag{6.3}$$

where $\bar{n} = \Psi_0^2 t_0$ is the parameter governing the system size expansion.

In the Wigner representation the evolution of the field $\phi(\xi, \tau)$ is governed by Eq. (6.2) with $s = 0$ provided the parameter $(\bar{n}^{-1/2})$ governing the system size expansion is sufficiently small that the third-order derivatives in the evolution equation for the Wigner function can be neglected. This means that the photon number of the quantized pump pulse has to be sufficiently large and the propagation distances sufficiently short ($\xi \ll \bar{n}^{1/2}$). This is in contrast to the positive-P representation for which Eq. (6.2) is exact (in the absence of boundary terms), since the Hamiltonian is only quadratic in boson creation operators for the sub-harmonic field and linear for the pump field. If the Hamiltonian does not include a quantized pump, then the dimensionless equations with $s = 0$ correspond exactly to the Fokker–Planck equation for $W$ and give identical results to the positive-P representation for a classical pump. We note that for the parametric amplifier there are no additional self-frequency shifts introduced by using the Wigner representation, as in the case of the quantum nonlinear Schrödinger equation [18]. In the Wigner representation the dynamics are restricted to the classical subspace $\{\phi^\dagger, \psi^\dagger\} = \{\phi^*, \psi^*\}$ so that the boundary conditions at $\xi = 0$ for a coherent state can be written (neglecting the nonzero mean amplitude) as $\phi(0, \tau) = \Delta\phi(0, \tau)$, $\psi(0, \tau) = \Delta\psi(0, \tau)$, and

$$\begin{aligned}\langle \Delta\phi(0,\tau)\Delta\phi^*(0,\tau')\rangle &= \frac{1}{2\bar{n}}\,\delta(\tau - \tau') \\ \langle \Delta\psi(0,\tau)\Delta\psi^*(0,\tau')\rangle &= \frac{1}{2\bar{n}}\left(\frac{\omega_2'}{\omega_1'}\right)\delta(\tau - \tau'),\end{aligned} \tag{6.4}$$

where $\Delta\phi$ and $\Delta\psi$ represent delta-correlated Gaussian stochastic processes with a mean of zero.

Using the semi-implicit integration method for Stratonovich stochastic differential equations described earlier, an algorithm can be constructed for the case of the $\chi^{(2)}$ interaction evolution equations. The positive-P stochastic equation for the field $\phi(\xi, \tau)$ driven by the pump field $\psi(\xi, \tau)$ is given by Eqs. (6.2). Neglecting the linear evolution for the moment and writing the field coordinate $\tau$ in discretized form, the stochastic integral for the interaction picture field $\phi_I$ (averaged over a transverse lattice cell at low transverse momentum) is

$$\begin{aligned}\phi_I(\xi_j + \Delta\xi, \bar{\tau}_m) - \phi_I(\xi_j, \bar{\tau}_m) \\ = \int_{\xi_j}^{\xi_j+\Delta\xi} d\xi' \int_{\tau_m}^{\tau_m+\Delta\tau} d\tau' [\phi_I^\dagger(\xi', \tau')\psi_I(\xi', \tau') \\ + \sqrt{\psi_I(\xi', \tau')}\zeta(\xi', \tau')]\end{aligned} \tag{6.5}$$

which is interpreted as the integral of a Stratonovich stochastic differential equation. In this case we could approximate the integral as

$$\phi_I(\xi_j + \Delta\xi, \bar{\tau}_m) - \phi_I(\xi_j, \bar{\tau}_m) = \phi_{jm}^\dagger \psi_{jm} \Delta\xi + \sqrt{\psi_{jm}}\Delta W_{jm}, \tag{6.6}$$

where the implicit approximation is used that the midpoint values can be calculated from

$$\phi_{jm} = \frac{1}{2}(\phi_I(\xi_j + \Delta\xi, \bar{\tau}_m) + \phi_I(\xi_j, \bar{\tau}_m)). \tag{6.7}$$

The noise terms have a correlation of

$$\langle \Delta W_{jm} \Delta W_{j'm'} \rangle = \frac{\delta_{j,j'}\delta_{m,m'}\Delta\xi}{\bar{n}\Delta\tau}. \tag{6.8}$$

The error in the drift component is improved to $O(\Delta\xi^3)$ by using these implicit midpoint estimates as explained earlier. In greater detail, the initial estimate of the midpoint is an Ito–Euler step of length $\Delta\xi/2$ given in the interaction picture by

$$\begin{aligned}\phi_{jm}^{(1)} &= \phi_I(\xi_j, \bar{\tau}_m) + (\phi_I^\dagger(\xi_j, \bar{\tau}_m)\psi_I(\xi_j, \bar{\tau}_m)\Delta\xi \\ &\quad + \sqrt{\psi_I(\xi_j, \bar{\tau}_m)}\Delta W_{jm})/2 \\ \psi_{jm}^{(1)} &= \psi_I(\xi_j, \bar{\tau}_m) - (\phi_I(\xi_j, \bar{\tau}_m))^2 \Delta\xi/4.\end{aligned} \tag{6.9}$$

The procedure for estimating the midpoint is iterated several times to improve convergence, as described earlier, together with similar equations for the fields $\phi^\dagger$, $\psi^\dagger$. After iteration to convergence, this provides the midpoint estimate for the semi-implicit step of length $\Delta\xi$, as

$$\begin{aligned}\phi(\xi_j + \Delta\xi, \bar{\tau}_m) &= \phi(\xi_j, \bar{\tau}_m) + \phi_{jm}^{(n)\dagger}\psi_{jm}^{(n)}\Delta\xi \\ &\quad + \sqrt{\psi_{jm}^{(n)}}\Delta W_{jm} \\ \psi(\xi_j + \Delta\xi, \bar{\tau}_m) &= \psi(\xi_j, \bar{\tau}_m) - (\phi_{jm}^{(n)})^2 \Delta\xi/2.\end{aligned} \tag{6.10}$$

After the interaction picture increment is calculated, the fields must be then propagated by linear transformations to the next cell location.

## VII. QUANTUM CORRELATIONS

### A. *Hybrid Wigner/Positive-P Simulations*

The correct quantum theory including a quantized pump is given by the positive-P representation, provided boundary terms are negligible. For highly non-classical states the doubled dimensionality of the phase-space can result in poor sampling statistics when calculating the squeezing spectrum. The Wigner representation on the other hand describes the dynamics exactly for a classical pump on the reduced phase-space where the stochastic fields representing the Hermitian conjugate field are in fact exactly the complex conjugate field. This fact can be utilized to provide a reference calculation for stochastic differencing, which significantly improves the sampling statistics for the positive-P calculation with a quantized pump.

Instead of directly calculating the squeezing spectrum including the effects of pump depletion and fluctuations in the positive-P representation, one calculates the difference between the squeezing spectrum for a classical undepleted pump and a quantized, depleted pump. The noise must be the same in both positive-P simulations. The Wigner representation is then used to calculate the squeezing spectrum for a classical undepleted pump which is exact, as explained above. The addition of the positive-P difference spectra and the Wigner spectra gives the correct quantum statistics including quantized pump. The important feature is that the sampling error is considerably smaller. The noise source for the Wigner representation is typically only in the initial conditions. However, for the positive-P representation noise needs to be generated at each space-time point, and the distribution function for a highly squeezed state is less compact than the Wigner distribution.

One can write down the appropriate reference stochastic equations as

$$\frac{\partial \phi_W}{\partial \xi} = -\frac{i}{2}\,\mathrm{sgn}(k_1'')\frac{\partial^2}{\partial \tau^2}\phi_W + \phi_W^* \psi_R$$

$$\begin{aligned}\frac{\partial \psi_R}{\partial \xi} = \Bigg[\frac{z_0}{t_0}\left(\frac{1}{\omega_1'} - \frac{1}{\omega_2'}\right)\frac{\partial}{\partial \tau} + iz_0(k_0^{(2)} - 2k_0^{(1)}) \\ - \frac{i}{2}\frac{k_2^{R\prime\prime}}{|k_1''|}\left(\frac{\omega_2'}{\omega_1'}\right)^2 \frac{\partial^2}{\partial \tau^2}\Bigg]\psi_R\end{aligned}$$

$$\frac{\partial \phi_R}{\partial \xi} = -\frac{i}{2}\,\mathrm{sgn}(k_1'')\,\frac{\partial^2}{\partial \tau^2}\,\phi_R + \phi_R^\dagger \psi_R + \sqrt{\psi_R}\,\zeta(\xi,\tau)$$

$$\frac{\partial \phi_R^\dagger}{\partial \xi} = +\frac{i}{2}\,\mathrm{sgn}(k_1'')\,\frac{\partial^2}{\partial \tau^2}\,\phi_R^\dagger + \phi_R \psi_R^* + \sqrt{\psi_R^*}\,\zeta^\dagger(\xi,\tau), \qquad (7.1)$$

where the classical undepleted pump $\psi_R$ has been utilized in the evolution of $\phi_R$, as well as in the Wigner calculation for $\phi_W$. These stochastic fields then correspond to different operator orderings and different dimensional phase-spaces. Solving these four additional reference equations as well as the original four equations can be more efficient than solving just the $(\phi, \phi^\dagger, \psi, \psi^\dagger)$ coupled positive-P equations alone.

B. *Squeezing Spectrum*

We treat ideal, pulsed, balanced, homodyne detection. The quantity needed for calculating the squeezing spectrum is given by the normally ordered and time-ordered operator expression [27]

$$2\pi\bar{n}^2\langle :\hat{X}_\theta(-\omega)\hat{X}_\theta(\omega):\rangle, \qquad (7.2)$$

where

$$\hat{X}_\theta(\tau) = \hat{\phi}^\dagger(\tau)\hat{\phi}_{LO}(\tau)e^{i\theta} + e^{-i\theta}\hat{\phi}_{LO}^\dagger(\tau)\hat{\phi}(\tau), \qquad (7.3)$$

where $\theta$ is an experimentally adjustable phase-shift, $\hat{\phi}_{LO}(\tau)$ is a pulsed local oscillator field operator, and $\hat{\phi}(\tau)$ is the signal field operator. The squeezing spectrum is optimized at each frequency by varying the local oscillator phase $\theta$. One can calculate correlation functions like Eq. (7.2) directly using the positive-P representation as ensemble averages correspond to normally ordered and time-ordered moments. It is convenient to calculate a normalized squeezing spectrum such that the minimum value of the correlation function is $-1$. In the positive-P representation

$$\langle X_\theta(-\omega)X_\theta(\omega)\rangle \geq -\frac{1}{2\pi\bar{n}}\left\langle \int d\tau\,(\phi_{LO}^\dagger\phi_{LO} + \phi^\dagger\phi)\right\rangle, \qquad (7.4)$$

where the brackets $\langle\ \rangle$ correspond to a stochastic average. Now the pulsed squeezing spectrum can be defined as

$$\begin{aligned} S_\theta(\phi,\xi,\omega) &= \langle \hat{S}_\theta(\phi,\xi,\omega)\rangle \\ &= \frac{2\pi\bar{n}\langle :\hat{X}_\theta(\xi,-\omega)\hat{X}_\theta(\xi,\omega):\rangle}{\langle \int d\tau\,(\hat{\phi}_{LO}^\dagger\hat{\phi}_{LO} + \hat{\phi}^\dagger\hat{\phi})\rangle}. \end{aligned} \qquad (7.5)$$

In the positive-P representation, the squeezing spectrum is then given by (including minimization w.r.t. $\theta$)

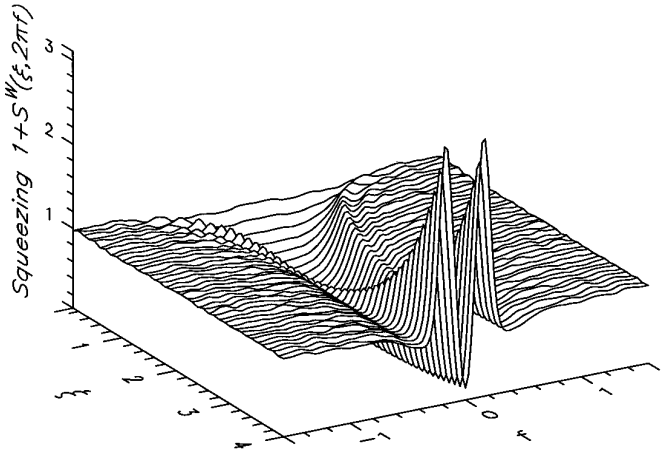


**FIG. 1.** Squeezing spectrum $1 + S^W(\phi_W, \xi, 2\pi f)$ versus propagation distance. This is a Wigner simulation of $\phi_W$ coupled to the classical pump field $\psi_R$ with the parameter values $\Delta k = 0$, $\mathrm{sgn}(k_1'') = 1$, $k_2^{Rr} = 0$, $\omega_1' = \omega_2'$, $\bar{n} = 10^{12}$ using 5000 trajectories. The initial conditions are $\phi$ in a vacuum state and $\langle\psi(0,\tau)\rangle = \mathrm{sech}^2(\tau/5)$, $\langle\phi_{LO}(\tau)\rangle = \mathrm{sech}(\tau/2)$.

$$\begin{aligned} S^P(\phi,\xi,\omega) &= \min_\theta\langle \hat{S}_\theta^P(\phi,\xi,\omega)\rangle \\ &= \frac{2\pi\bar{n}\,\min_\theta\langle X_\theta(\xi,-\omega)X_\theta(\xi,\omega)\rangle}{\langle \int d\tau\,(\phi_{LO}^\dagger\phi_{LO} + \phi^\dagger\phi)\rangle}. \end{aligned} \qquad (7.6)$$

In the Wigner representation, the stochastic moments correspond to symmetrical operator ordering resulting in the stochastic moment $\langle X_\theta(-\omega)X_\theta(\omega)\rangle$ being non-negative. The squeezing spectrum in the Wigner representation is then

$$S^W(\phi,\xi,\omega) = -1 + \frac{2\pi\bar{n}\,\min_\theta\langle X_\theta(\xi,-\omega)X_\theta(\xi,\omega)\rangle}{\langle \int d\tau\,[|\phi_{LO}|^2 + |\phi|^2 - 1/(\bar{n}\Delta\tau)]\rangle}, \qquad (7.7)$$

where $\Delta\tau^{-1}$ is the frequency cut-off. The hybrid spectrum is constructed from

$$\begin{aligned} S^{HYBRID}(\xi,\omega) = \langle \hat{S}^P(\phi,\xi,\omega) - \hat{S}^P(\phi_R,\xi,\omega)\rangle \\ + S^W(\phi_W,\xi,\omega). \end{aligned} \qquad (7.8)$$

To illustrate the effectiveness of the algorithm simulation, results for quantum field propagation in a $\chi^{(2)}$ waveguide are given for a case where there is a substantial difference between the choice of $S^W(\phi_W, \xi, \omega)$ and physically measured spectrum $S_\theta(\phi, \xi, \omega)$. Figure 1 shows the squeezing spectrum $S^W(\phi_W, \xi, \omega)$ calculated using the Wigner representation. The corresponding DC component is shown in Fig. 3. The estimated sampling error for the DC component was much smaller than either the high-frequency components or the positive-P sampling errors. The estimated lattice error for the DC component was smaller than the

sampling error. The difference spectrum $\langle \hat{S}^P(\phi, \xi, \omega) - \hat{S}^P(\phi_R, \xi, \omega)\rangle$ is shown in Fig. 2 and the corresponding DC component in Fig. 3. The DC component of the hybrid spectrum $S^{HYBRID}(\xi, \omega)$ and its estimated sampling error are also given in Fig. 3. For comparison, a positive-P simulation of comparable execution time to the hybrid scheme was performed and its DC component is given in Fig. 3 as well. The convergence in the latter case is very poor as a function of the number of trajectories. Figure 3 shows that the hybrid scheme is considerably better even when there is a large difference between the calculated Wigner result and the full positive-P result. In fact, for the parameters used here the hybrid scheme can give the correct quantum statistics with estimated errors many orders of magnitude less than shown in Fig. 3 by including the pump dispersion in the evolution of $\psi_R$. It is often the case that the sampling error away from DC using the Wigner representation is larger than for a corresponding positive-P simulation. This example illustrates that the reference calculation used in the stochastic differencing scheme need not have a smaller sampling error for all momentum space but just the subspace of interest.

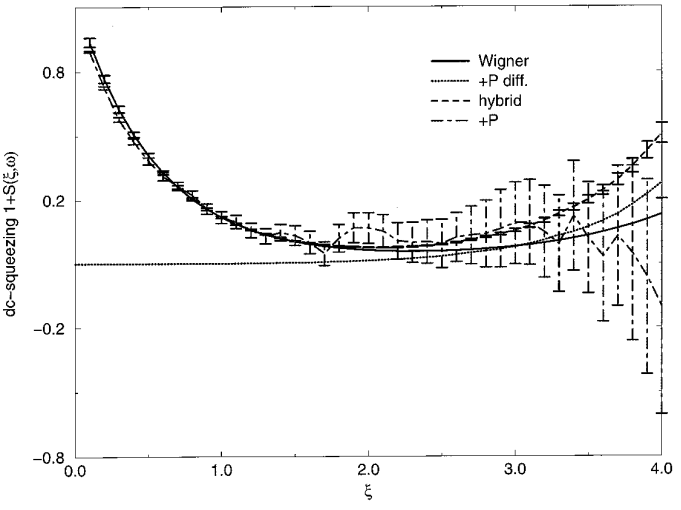


**FIG. 3.** DC squeezing versus propagation distance for the Wigner simulation in Fig. 1, positive-P difference simulation in Fig. 2, hybrid method and positive-P simulation in Fig. 4. The estimated errors for the Wigner and positive-P difference simulations are not shown here. However, for the simulations shown here the error estimates for the hybrid case are essentially the same as in the positive-P difference simulation.

## VIII. ENSEMBLE AVERAGES AND MIMD APPROACH

Ensemble averages of stochastic quantities requires an understanding of operator ordering for the physically relevant quantum mechanical averages to be calculated correctly. In addition, there is the need for statistical confidence intervals to be inferred in order to ascertain the reliability of the predictions. The calculations are completed in a three stage process which is more clearly defined in the case of a distributed computing model. Initially, averages over each sub-ensemble are made for the stochastic equivalent of the operator products of interest. The plotted data correspond to the mean over all trajectories for each expectation value expression evaluated on the fine lattice.

In order to estimate errors, the following sub-ensemble averages are made. For simple quantities such as intensity the data are simply the average over all sub-ensembles of a single operator product equivalent and are therefore identical to a direct average over all trajectories. For more complicated quantities such as squeezing spectra, these involve combinations of expectation values of different operator products. In this case, the data are the average

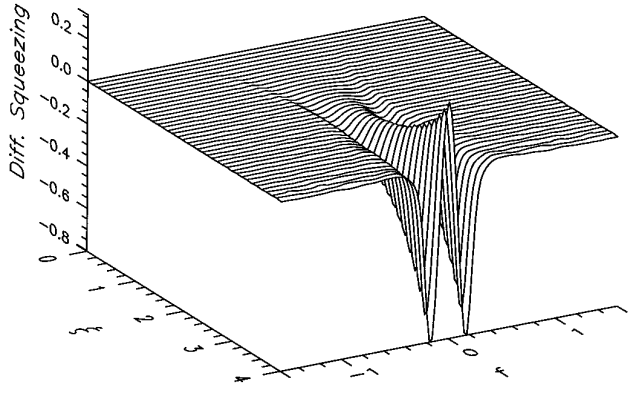


**FIG. 2.** Difference squeezing spectrum versus propagation distance using the positive-P fields $\phi$, $\phi_R$, $\psi$. The initial conditions and parameters are the same as in Fig. 1 except that $k_2'' = k_1''$.

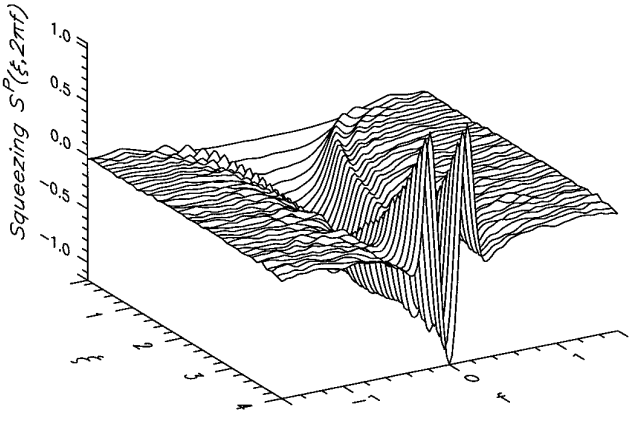


**FIG. 4.** Squeezing spectrum $S^P(\phi, \xi, 2\pi f)$ versus propagation distance. This is a positive-P simulation with the parameter values the same as for $\phi$ in Fig. 3 using 10,000 trajectories. The initial conditions are the same as in Fig. 1.

over sub-ensembles of functions of sub-ensemble averaged operator product equivalent stochastic quantities. From this there are two error estimates provided, one based on results from different lattices and one on the number of sub-ensembles. Assuming a Gaussian stochastic process, an estimate of the standard error is given as the square root of the variance divided by the sample population minus one, i.e., one less than the number of sub-ensembles. Since the mean is evaluated on the fine lattice, the variance also corresponds to those trajectories integrated over the fine lattice. The absolute value of the difference between mean values evaluated over the coarse and fine lattices provides an estimate of the lattice error.

A stochastic description of the evolution of fields has an implicit parallelism. Moreover, using such a representation allows the expectation values of operators to have an explicit correspondence to ensemble averages of stochastic trajectories. Herein lies the appeal of a divide-and-conquer parallel algorithm—each trajectory is independent of each other and therefore can be calculated on a remote node without any inter-node communication. The general principle of divide-and-conquer is implemented with the PVM (Parallel Virtual Machine) package [14]. It is a message passing system designed to allow a heterogeneous network of machines to complete a task in parallel. The initial value problem is of the type given by Eq. (1.1). One can associate a trajectory of a stochastic process for each instance of an initial condition. These initial conditions may be all the same or can be described by a probability distribution. As all trajectories are independently propagated they could be initiated at the same time on different machines or whatever is appropriate for the architecture in use. The ensemble is divided into $\sqrt{\mathcal{N}}$ sub-ensembles which allows a number of features to be implemented easily. Firstly, some measure of statistical error from using a finite sample size can be estimated. Secondly, fault tolerance can be built into the scheduling algorithm such that one can lose at most one sub-ensemble of data per node failure.

On an IBM SP2 with a high-performance switch, dedicated use of the node pool (say $\mathcal{M}$ nodes) allows static load-balancing so a slave is spawned on each node where each slave calculates at least $\gcd(\sqrt{\mathcal{N}},\mathcal{M})$ sub-ensembles. The code has also been implemented on shared-memory processors and clusters of workstations. In both these cases a simple form of dynamic load-balancing using the pool of tasks paradigm for scheduling has been implemented. Each slave process is capable of calculating any number of the $\sqrt{\mathcal{N}}$ sub-ensembles. This flexibility is used by the scheduler to take into account the estimated speed of the processor/memory subsystems important for load-balancing in a heterogeneous cluster. Initially, tasks are spawned on each machine's processor set with each slave passed a message containing the parameter set for the physical problem, a RNG seed and the number of sub-ensembles to compute. As a task is completed by node it is sent another one immediately if there has been less than $\sqrt{\mathcal{N}}$ tasks successfully allocated. A simple form of fault-tolerance is included by checking for the number of nodes removed from the virtual machine after $\sqrt{\mathcal{N}}$ sub-ensembles have been allocated. If nodes have been removed then additional slaves are spawned on a round-robin basis to the available nodes until $\sqrt{\mathcal{N}}$ sub-ensembles have been successfully computed. Hence, the limiting speed is the time taken to initiate and retrieve a single sub-ensemble from the slowest node in the cluster and output the results. Therefore, use of such a simple scheduling algorithm requires a careful choice of the nodes forming the cluster.

## IX. CONCLUSIONS

A family of algorithms for the integration of stochastic parabolic partial differential equations has been presented, together with techniques for improving the discretization and sampling errors. An example application involving experimentally measurable correlation functions for one dimensional propagating quantum fields has been shown in detail. Calculation of correlation functions of interacting stochastic fields has been discussed. An efficient approach for overcoming sampling errors with the use of a non-diagonal coherent state representation for studying quantum field propagation in dispersive nonlinear dielectrics has been presented. It has been shown that it is sometimes more efficient to solve the exact positive-P stochastic equations in combination with an exact Wigner representation of a related problem. It is expected that these techniques will be useful for studying higher-order quantum correlation functions, as well as other related systems described by the use of stochastic partial differential equations.

## REFERENCES


1. H. Haken, *Synergetics*, (Springer-Verlag, New York/Berlin, 1978).
2. H. Risken, *The Fokker-Planck Equation—Methods of Solution and Applications*, 2nd Ed. (Springer-Verlag, New York/Berlin, 1989).
3. C. W. Gardiner, *Handbook of Stochastic Methods for Physics, Chemistry and the Natural Sciences,* corrected 2nd ed. (Springer-Verlag, New York/Berlin, 1990).
4. S. K. Ma, *Modern Theory of Critical Phenomena* (Benjamin, Elmsford, NY, 1976).
5. C. W. Gardiner, *Quantum Noise* (Springer-Verlag, New York/Berlin, 1991).
6. S. J. Carter, P. D. Drummond, M. D. Reid, and R. M. Shelby, *Phys. Rev. Lett.* **58,** 1841 (1987); P. D. Drummond and S. J. Carter, *J. Opt. Soc. Am. B* **4,** 1565 (1987); P. D. Drummond, R. M. Shelby, S. R. Friberg, and Y. Yamamoto, *Nature* **365,** 307 (1993); S. J. Carter and P. D. Drummond, *Phys. Rev. Lett.* **67,** 3757 (1991).
7. L. A. Lugiato and I. Marzoli, *Phys. Rev. A* **52,** 4886 (1995).
8. M. H. Anderson, J. R. Ensher, C. E. Wieman and E. A. Cornell, *Science* **269,** 198 (1995); C. C. Bradley, C. A. Sackett, J. J. Tollett, and R. G. Hulet, *Phys. Rev. Lett.* **75,** 1687 (1995); K. B. Davis,

M. O. Mewes, M. R. Andrews, N. J. van Druten, D. S. Durfee, D. M. Kurn and W. Ketterle, *Phys. Rev. Lett.* **75,** 3969 (1995); K. Burnett, *Contemp. Phys.* **37,** 1 (1996); K. B. Davis, M. O. Mewes and W. Ketterle, *Appl. Phys. B* **60,** 155 (1995).

9. P. D. Drummond and I. K. Mortimer, *J. Comput. Phys.* **93,** 144 (1991).
10. P. E. Kloeden and E. Platen, *Numerical Solution of Stochastic Differential Equations* (Springer-Verlag, New York/Berlin, 1992).
11. P. D. Drummond, *Comput. Phys. Commun.* **29,** 211 (1983).
12. N. Nagase, *SIAM J. Control Optim.* **33,** 1716 (1995).
13. M. SeeBelberg and F. Petruccione, Comput. Phys. Commun. **74,** 303 (1993).
14. A. Geist, A. Beguelin, J. Dongarra, W. Jiang, R. Manchek, and V. S. Sunderam, *PVM*: *Parallel Virtual Machine a User's Guide and Tutorial for Networked Parallel Computing* (MIT Press, Cambridge, MA, 1994).
15. G. N. Milstein, Theory Probab. Appl. **19,** 557 (1974).
16. K. Ito, *Lectures on Stochastic Processes* (Tata, Bombay, 1960).
17. W. H. Press, S. A. Teukolsky, W. T. Vetterling, and B. P. Flannery, *Numerical Recipes in FORTRAN*: *The Art of Scientific Computing*, 2nd ed. (Cambridge Univ. Press, Cambridge, UK, 1992).
18. P. D. Drummond and A. D. Hardman, *Eur. Lett.* **21,** 279 (1993).
19. M. J. Werner, *Phys. Rev. A* **54,** R2567 (1996); S. R. Friberg, S. Machida, M. J. Werner, A. Levanon, and Takaaki Mukai, *Phys. Rev. Lett.* **77,** 3775 (1996).
20. M. J. Werner, M. G. Raymer, M. Beck, and P. D. Drummond, *Phys. Rev. A* **52,** 4202 (1995).
21. G. Marsaglia, A. Zaman, and W. W. Tsang, *Statist. Probab.Lett.* **8,** 35 (1990).
22. M. G. Raymer, P. D. Drummond, and S. Carter, *Opt. Lett.* **16,** 1189 (1991).
23. P. D. Drummond and S. J. Carter, *J. Opt. Soc. Am. B* **4,** 1565 (1987).
24. K. E. Cahill and R. J. Glauber, *Phys. Rev.* **177,** 1882 (1969).
25. M. J. Werner and H. Risken, *Phys. Rev. A* **44,** 4623 (1991).
26. P. D. Drummond and C. W. Gardiner, *J. Phys. A* **13,** 2353 (1980).
27. P. D. Drummond, S. J. Carter, and R. M. Shelby, *Opt. Lett.* **14,** 373 (1989).